Proceedings of the
44th IEEE Conference on Decision and Control, and
the European Control Conference 2005
Seville, Spain, December 12-15, 2005

D-OSKIL: a New Mechanism for Suppressing Stick-Slip in Oil Well Drillstrings

Carlos Canudas-de-Wit, Miguel A. Corchero, Francisco R. Rubio and Eva Navarro-López

Abstract— **Limit cycles occurring in oil well drillstrings result from the interaction between the drill bit and the rock during drilling operations. In this paper we propose to use the weight on the bit (WoB) force as an additional control variable to extinguish limit cycles if they occur. In particular we adapt the *oscillation killer* (OSKIL) mechanism studied in detail in the companion paper [3] to our problem at hand. An approximate analysis based on the bias describing function and completed with some simulations, provides good evidences that the rotational dynamics of the oil well drillstring display such a behavior. Simulations applying the D-OSKIL (D stands for Drilling) mechanism show that the stick-slip oscillations can be eliminated without requiring a re-design of the velocity rotary-table control.**

Index Terms— **Stick-Slip Elimination, Oil Well Drillstring, OSKIL.**

I. Introduction

Oilwell drillstrings are systems which present interesting features from the dynamical and control viewpoints. The presence of stick-slip self-excited oscillations at the bottom part of drillstrings has attracted the attention of the control community in the last decade. The elimination of this kind of oscillations is a challenge for drillers and scientists. The fact of reducing these oscillations can give important cost savings in drilling operations.

Different oscillations affect the drillstring behavior. This paper is focused on stick-slip oscillations given at the bottom-hole assembly (BHA), i.e., the top of the drillstring rotates with a constant rotary speed, whereas the bit (cutting device) rotary speed varies between zero and up to six times the rotary speed measured at the surface. Stick-slip oscillations are mainly due to the friction interface between the BHA and the rock formation [9]. Consequently, a model describing the drillstring behavior should include the bit-rock friction effect. A lumped parameter model is used in this paper. The drillstring is considered as a torsional pendulum with two degrees of freedom, as shown in Figure 1.

There are several alternatives when considering the problem of suppressing stick-slip oscillations. One possibility is to manipulate the different drilling parameters such as: increasing the rotary speed, decreasing the weight-on-bit (WoB), modifying the drilling mud characteristics, or introduction of an additional friction at the bit [13]. These strategies, although not supported by formal analysis, have been shown in the field to be effective to suppress stick-slip motion [14].

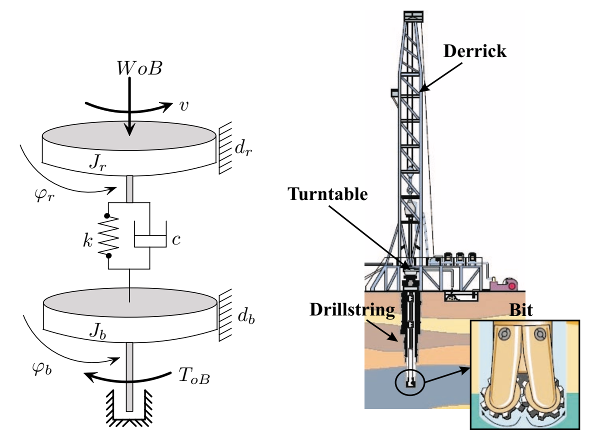

Fig. 1. Simplified model of an oilwell drillstring (left) and a vertical rotary-drilling real equipment (right)

Another alternative has been the introduction of new control methodologies (active, passive) to compensate drillstring stick-slip vibrations. Among them we have: the *soft torque rotary system* (STRS) introduced in [7],[14]; the use vibration absorber at the top of the drillstring [8], [7], [14]; the design of reduced-order PID rotary speed controllers [1], [12], [13]; the design of linear H_∞ controllers [15]. More recently, the manipulation of the normal force regarded as WoB has been shown to play an important role in reducing stick-slip oscillations [12].

In this paper, using the weight on the bit (WoB) force as an additional control variable is proposed. In particular we adapt the *oscillation killer* (OSKIL) mechanism studied in detail in the companion paper [3], to the oil well drillstring systems (named here D-OSKIL[1]) which has been shown to be particulary adapted for nonlinear systems displaying a local stable region with an stable limit set outside this local domain. An approximate analysis based on the bias describing function provides good evidences that the rotational dynamics of the oil well drillstring display a similar behavior. This analysis, although approximative, also gives a good intuition in the way that the WoB needs to be modified to suppress oscillations. An important property

C. Canudas-de-Wit is with The Laboratoire d'Automatique de Grenoble, UMR CNRS 5528, ENSIEG-INPG, B.P. 46, 38 402, ST. Martin d´Hères, FRANCE. On leave at the University of Seville (Sept.04 till June 05). Email: carlos.canudas-de-wit@inpg.fr.
Miguel A. Corchero and Francisco R. Rubio are with the Escuela Técnica Superior de Ingenieros, University of Seville, Camino de los Descubrimientos s/n, 41092-Sevilla, SPAIN. Email: macperu@cartuja.us.es,rubio@esi.us.es.
E. Navarro-López is with the Instituto Mexicano del Petróleo, Eje Central Lázaro Cárdenas, 152, ed. 2, planta baja, cub.1, A.P. 14-805, 07730 México, D.F., México. Email: navarro.lopez@gmail.com.

[1]D-OSKIL stands for Drilling oscillation killer mechanism.

of the proposed D-OSKIL mechanism is that allows to recover the nominal operation condition (the WoB recovers its nominal drilling value) while oscillations are suppressed. Simulations applying the D-OSKIL mechanism show that the stick-slip oscillations can be eliminated in that way without requiring a re-design of the velocity rotary-table control.

II. Drillstring model

Multiple kind of models have been used in literature to describe these systems (for example; [10] and [16]). Lumped parameters models have been shown valid enough to describe properly the stick-slip oscillation phenomena and easy enough to make the study not too complex ([6]). Different bit-rock friction models are presented in [11].

The model used here (see Figure 1) is a two-degree-of-freedom model with two inertial masses J_r and J_b, locally damped by d_r and d_b. The inertias are coupled each other by an elastic shaft with stiffness k and damping c. The variables φ_r and φ_b stand for the rotary and the bit angles. The T_{oB} (Torque on Bit) represents the total friction torque over the drill bit and v is the rotary torque control signal used to regulate the rotary angular velocity $\dot{\varphi}_r$. The model equations are:

$$\begin{aligned} J_r\ddot{\varphi}_r + c(\dot{\varphi}_r - \dot{\varphi}_b) + k(\varphi_r - \varphi_b) + d_r\dot{\varphi}_r &= v \\ J_b\ddot{\varphi}_b + c(\dot{\varphi}_b - \dot{\varphi}_r) + k(\varphi_b - \varphi_r) + d_b\dot{\varphi}_r &= -T_{oB} \end{aligned}$$

In constants above, the sub-script $'r'$, and $'b'$ stands for rotary and bit, respectively.

The T_{oB} is given by the product between $\mu(\dot{\varphi}_b, z)$, which describes the normalized (dimensionless) torsional bit-rock friction, and the normal force u usually named the Weight on Bit (WoB), i.e.

$$T_{oB} = \mu(\dot{\varphi}_b, z) \cdot u, \qquad u = u_0 + \tilde{u}$$

The effective value of T_{oB} can be modified by controlling the tension force, $\tilde{u}$, of the drillstring. We assume that a counterweight force $\tilde{u} \in [-u_0, 0]$ can be applied to counteract the nominal force $u_0 = Mg$ (this is the gravitational normal force due to the total drillstring mass M time the gravity g), with a trivial minimum of $-u_0$.

This lumped model has the following state-space representation:

$$\begin{aligned} \dot{x} &= Ax + Bv + H\mu(x, z)u & (1) \\ \dot{z} &= f(x, z) & (2) \end{aligned}$$

with

$$A = \begin{pmatrix} 0 & 1/i & -1 \\ -k/iJ_r & -(d_r + c/i^2)/J_r & c/iJ_r \\ k/J_b & c/iJ_b & -(c + d_b)/J_b \end{pmatrix}$$

$$B^T = \begin{pmatrix} 0 & 1/J_r & 0 \end{pmatrix}, \quad H^T = \begin{pmatrix} 0 & 0 & -1/J_b \end{pmatrix}$$

where the state $x = [x_1, x_2, x_3]^T$ is defined as: $x_1 = \frac{\varphi_r}{i} - \varphi_b$, $x_2 = \dot{\varphi}_r$, and $x_3 = \dot{\varphi}_b$. i is the rotation ratio. In this description, the state $z \in R$ represents the internal friction state, and Equation (2) describes the friction dynamics. One possible model for (2) is the *LuGre* friction model ([5]):

$$\begin{aligned} \dot{z} &= x_3 - \sigma_0 \frac{|x_3|}{g(x_3)} z, \\ g(x_3) &= \mu_C + (\mu_S - \mu_C)e^{-(x_3/v_s)^2} & (3) \\ \mu(x, z) &= \sigma_0 z + \sigma_1 \dot{z}, \end{aligned}$$

Note that the torsional linear friction at the drill bit side is already incorporated in the A matrix of the representation (1). $\sigma_0, \sigma_1, v_s, \mu_C, \mu_S$ are positive constants characterizing the friction physical properties. Realistic values for parameters (see [15]) are given in the Appendix A.

III. Velocity-controlled drillstring

Without loss of generality, it is assumed that the state x is measurable[2]. A velocity control-loop (static or dynamic) is then first designed to regulate the output rotary velocity $\dot{\varphi}_r$ to some desired value ω_d (a typical value for ω_d is $5\,rad/s$).

Although many velocity control structures are possible, oil well drilling often operates with reduced-order simple control laws.

A common control structure [6] is:

$$v = \left[k_1 + \frac{k_2}{s}\right](\omega_d - \dot{\varphi}_r) - k_3(\dot{\varphi}_r - \dot{\varphi}_b) \qquad (4)$$

or equivalent

$$\begin{aligned} v &= k_1(\omega_d - x_2) + k_2 x_4 - k_3(x_2 - x_3) \\ \dot{x}_4 &= \omega_d - x_2 \end{aligned}$$

then the closed-loop equations take the form,

$$\begin{aligned} \dot{x} &= A_{cl}x + B_{cl}\omega_d + H_{cl}\mu(x, z)u & (5) \\ \dot{z} &= f(x, z) & (6) \end{aligned}$$

with the obvious observation that the state is now of dimension four, i.e. $x = [x_1, x_2, x_3, x_4]$, and with the A_{cl}, B_{cl} and H_{cl} defined accordingly.

The gains values can be designed using pole placement. For instance, the first pair of poles are set as a pair of complex-conjugate poles with frequency ω_n and damping ratio δ. The second pair can be placed at $1.5\,\omega_n$ and $6\,\omega_n$. This configuration will allow to study the system behavior for different combinations of ω_n and WoB.

It is assumed that for certain values of the gains and the WoB, the drillstring system enters into sustained oscillation, and cases where the drill bit rotational velocity reaches the desired stable equilibrium point (see for instance Figure 7).

This behavior is shown in Figure 2, where the WoB parameter is perturbed away from its nominal operation value; in Figure 2-(a), the WoB changes from $40000N$ to $45000N$ and the controller is still able to correctly regulate the rotatory speed (the state does not leave its local attraction domain), whereas in Figure 2-(b) the WoB is perturbed enough (from $40000N$ to $50000N$) so that the states are

[2] The problem can be also formulated including an observer. An observer may be needed because the bit velocity is not generally sensed

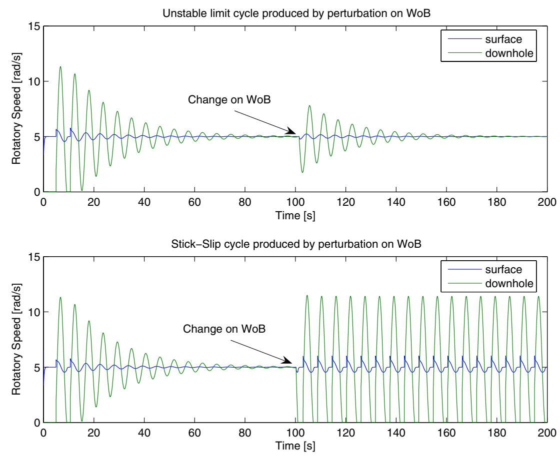

Fig. 2. Different behaviors obtained by perturbing WoB: (a) states are attracted by its local stable equilibrium (upper), (b) states are attracted by the limit cycle (lower).

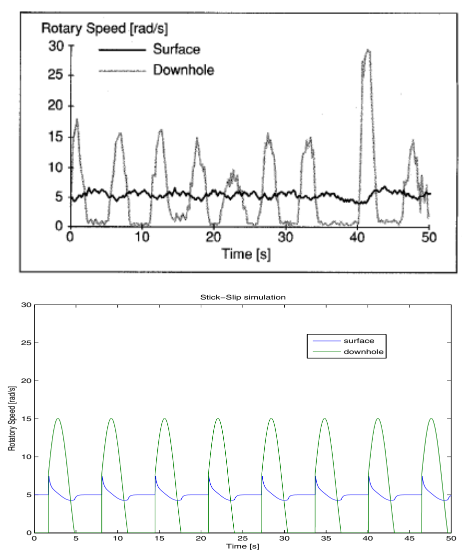

Fig. 3. Stick-slip measured in the field (upper), reproduced with permission from [15], and simulation profiles obtained with the 2-d.o.f. lumped model in closed-loop (5)-(6)(lower).

attracted by an stable limit cycle. In this latter case the velocity controller cannot compensate the perturbation and the system enters into stick-slip oscillation.

In Figure 3 can be seen a comparison between stick- slip oscillations measured in the field[3] and the ones produced by simulating the closed-loop system (5)-(6). Note that, although the model does not include the lateral and vertical motion dynamics, it is able to reproduce trajectories that are qualitatively close to the ones reported from field data.

IV. Stick-slip oscillations prediction based on DF-analysis

The pattern of the oscillation shown by Figure 3 reflects two main characteristics: first oscillations will present a bias term, and second they are dominated by a main harmonic with relatively well defined period. Therefore, the SBDF (Sinusoid plus bias describing function) method can then be used as a first approximation to predict possible limit cycle and to study its stability. To simplify further the computation of the SBDF corresponding to the nonlinear dynamic friction map (3), we rather use a simpler approximation of the resulting steady-state characteristic of (3), see Figure 4. This approximation is valid because the friction dynamics is much faster than the one of the drillstring mechanism.

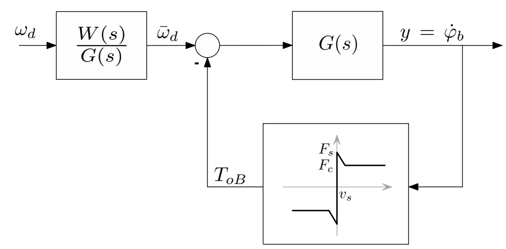

Fig. 4. System block diagram and static friction torque.

The setup for this study is shown in Figure 4. $G(s)$ is the linear map from $G(s) : (\bar{\omega}_d - ToB) \rightarrow y = \dot{\varphi}_b$, and $\bar{\omega}_d$ is the resulting bias due to the constant reference ω_d.

Applying harmonic balance, the necessary condition to produce maintained oscillations in the system is:

$$G(j\omega_0) = \frac{-1}{N_1(A_0, \omega_0, y_0)} \quad (7)$$

$$y_0 \left[1 + G(0)N_0(A_0, y_0)\right] = W(0)\omega_d \quad (8)$$

A_0 and ω_0 are the particular values satisfying both equalities. They represent the amplitude and frequency of the predicted oscillations, if any. y_0 is the output bias, and N_1 and N_0 are given in the report [4].

Note that $G(j\omega)$ depends on the control parameters, hence on the assigned bandwidth ω_n. The Nyquist diagram of $G(j\omega)$ is shown in Figure 5 as a function of ω_n. The arrows indicate the sense of increasing ω_n. It is interesting to notice that $G(j\omega)$ changes sign twice as ω_n increases.

For small ω_n, the map G is in the right half-plane. Increasing ω_n, $G(j\omega)$ increases its magnitude until its Nyquist goes into the left half-plane. A further increase of ω_n makes $G(j\omega)$ to stretch in magnitude until its sign changes again. Table I gives the domain for ω_n, as a function of the location of the Nyquist of $G(j\omega)$.

TABLE I
Situation of Nyquist diagram of $G(j\omega)$ as a function of ω_n.

ω_n	Situation
$[0, 2.85]$	Right half-plane
$[2.85, 12.01]$	Left half-plane
$[12.01, \infty]$	Right half-plane

Since the observed oscillations are clearly asymmetrical, the SBDF is used to compute $N_1(A, \omega, y_0)$, see [2]. $N_1(A, y_0)$ will have only real part since the friction torque characteristic has odd symmetry.

[3]Figure obtained from [15]

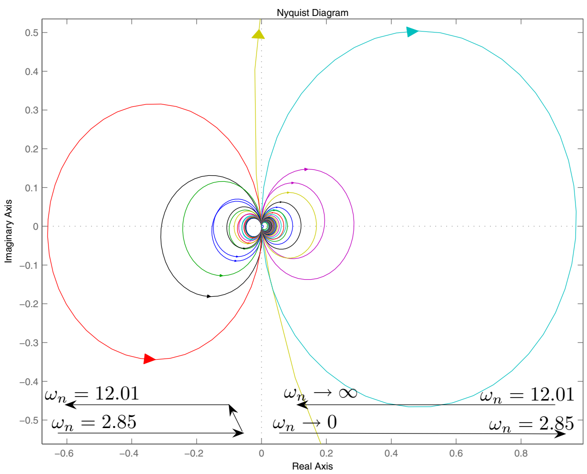

Fig. 5. Nyquist diagram of G for different values of ω_n.

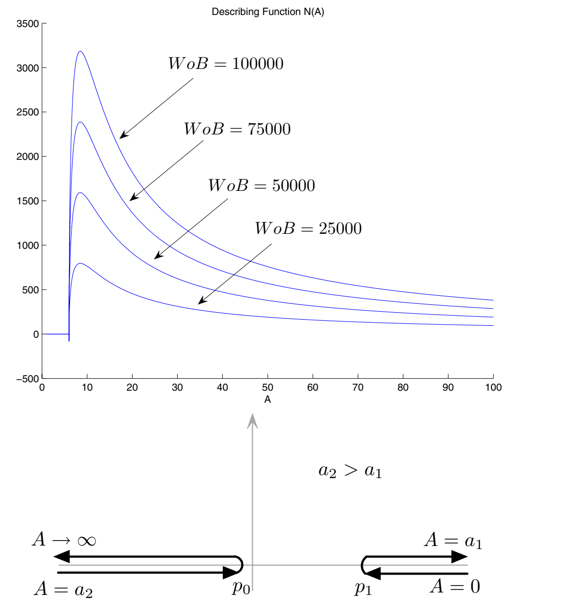

Fig. 6. Describing function $N(A)$ (upper), and evolution of $\frac{-1}{N(A)}$ (lower). $|p_0|$ is two or three magnitude orders lower than $|p_1|$, depending on value of WoB.

Note that the frequency locus of $G(j\omega_0)$ can only cross the real axis in one point, then ω_0 can be uniquely computed from $\mathcal{I}m\{G(j\omega_0)\} = 0, \ \forall \ \ \omega_0 \neq 0, \ \ |\omega_0| < \infty$, and hence does not depend on the other two unknown variables A_0 and y_0. The introduction of a integral action in the velocity control results in $G(0) = 0$, and $W(0) = 1$. Therefore, the output bias can be straightforwardly computed from equation (8). Yielding

$$y_0 = \frac{W(0)}{[1 + G(0)N_0(A_0, y_0)]}\omega_d = \omega_d$$

With $y_0 = \omega_d$ known and independent of frequency and the amplitude, the prediction of the limit cycle and its associated amplitude A_0, can be obtained only from equation (7), i.e.

$$\mathcal{R}e\{G(j\omega_0)\} = -\frac{1}{N(A_0)}$$

with $N(A_0) = N_1(A, \omega_d)$.

Figure 6 shows how $\frac{-1}{N(A)}$ changes as a function of A. The main feature of this amplitude locus, pertinent to oscillations prediction, is the location of points p_0 and p_1. These points derive from the maximum and minimum values of $N(A)$. In particular, it is interesting to notice that these points have the following property:

$$|p_0| \sim \frac{1}{WoB} \qquad \text{and} \qquad |p_1| \sim \frac{1}{WoB}$$

Then, low values of WoB makes these two points bigger in magnitude (its sign remains unchanged), reducing the possibility to intersect the Nyquist of $G(j\omega)$. Inversely, when the weight on bit force increases, the probability to get an oscillation is higher.

It is also interesting to note, that for almost every realistic choice of ω_n, two sets of limit cycles will be predicted; one stable set and another unstable. The stable set arises at amplitudes $A = A_s$, whereas the unstable one occurs for $A = A_u$. In all cases $A_s > A_u$. This means that for all parameter combination $(WoB - \omega_n)$ where an intersection of $G(j\omega)$ and $-1/N(A)$ takes place, there exists a local (attractive) stable domain delimited by A_u. This property is exploited further in the proposed D-OSKIL mechanism.

It is also of interest to compute the set of possible combination between system bandwidth and weight on bit force for which stable limit cycles are predicted. Figure 7 shows the zone in the $(WoB - \omega_n)$-plane giving rise to possible stable oscillations. This analysis allows to determine the range of proper values of controller closed-loop bandwidth to avoid oscillations as a function of the operating WoB. As the figure shows, and on the basis of this analysis, oscillations may be eliminated either by changing ω_n, and/or by reducing the WoB magnitude.

One possible control strategy could be then to modify the rotary table bandwidth to reduce the possibility to enter into oscillation. From Figure 7, we can see that suitable choices for ω_n are either small or large values. Small values are not suited because yield to poor performance, and large values are limited by noise. Typical values for ω_n are in the range $[20, 30]\,rad/s$.

Another alternative will be to keep the value of WoB below the oscillation zone. However, this will have two drawbacks: first, high-performance drilling operation requires magnitudes for WoB larger than the ones indicated by the oscillation limits, and second this strategy will require a precise knowledge of this map, which in addition will vary as a function of the drilling depth. Keeping WoB low, will thus be a too conservative strategy.

High-performance drilling operation takes place in a region in the plane $(WoB - \omega_n)$, where potential oscillations may occur. Therefore, in this paper we account for this particularity assuming that the *nominal* system operation parameters are taken within this zone. The control strategy presented next, is thus built under the following base-lines:

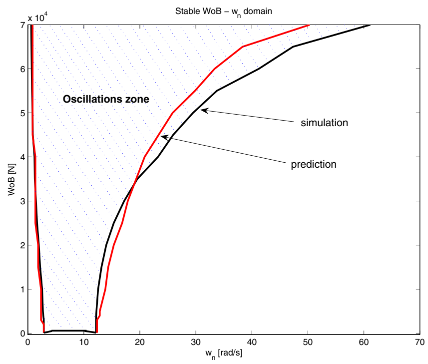

Fig. 7. Oscillations frequency domain. Border obtained by simulations and border predicted from the SBDF analysis.

- *nominal* values for $(WoB - \omega_n)$ are in the potential stable limit cycle zone. Then, stick-slip limit cycles are possible under a substantial perturbation.
- oscillation will be eliminated by decreasing the Weight on Bit force. In other words, by reducing the WoB, the local attraction domain is enlarged about the equilibrium points, until system trajectories are attracted to them. This effect is understandable from Figure 7.
- after that, the WoB will have to be set to its nominal value again to continue properly with the drilling task. This is not seen directly from Figure 7. However, this is possible as long as the system trajectories are kept within the local attraction domain, by a slow variation of the WoB, see [3]

V. The D-OSKIL: Drilling Oscillation Killer Mechanism

The OSKIL mechanism has been designed (see detail in the companion paper [3]) assuming that originally the WoB is set to its nominal value ($u = u_0$). Further, we assume the nominal system parameter operation, in term of values for $(WoB-\omega_n)$, is due inside potentially oscillation zone shown in Figure 7, but system trajectories are at its equilibrium, i.e. $\dot{\varphi}_r = \omega_d$. However, as it is often the case during the drill operation, variation on the rock friction characteristics may bring the closed-loop system trajectories outside the local stable zone producing stick-slip cycles.

The problem is thus to modify (temporally) the effective value of u via the additional control signal $\tilde{u}$ as shown in the representation (1), so that the oscillations can be eliminated, while bringing back the effective value of u to its nominal operation value, u_0. One possible structure for the D-OSKIL mechanism is the following one:

$$y = Cx = \dot{\varphi}_b \quad (9)$$

$$y_f = F(s)y \quad (10)$$

$$\xi = \int_t^{t+T} y_f^2(\tau)d\tau \quad (11)$$

$$\frac{1}{\sigma}\dot{\tilde{u}} = -\tilde{u} - \mathrm{sat}_0^{u_0}(K_I\xi), \quad \tilde{u}(0) = 0 \quad (12)$$

$$u = u_0 + \tilde{u} \quad (13)$$

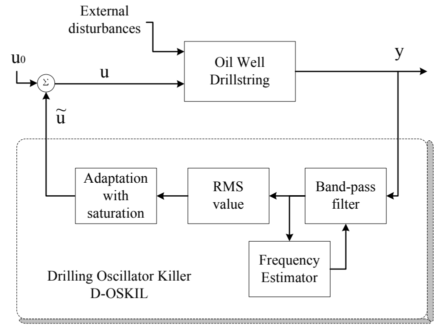

Fig. 8. Block scheme of the oscillation killer control.

- Equation (9) selects a suitable output reflecting the stick-slip oscillations. This choice is not unique, and it may depend on the signal-to-noise ratio of the considered output. To simplify matters, the selected output is $y = \dot{\varphi}_b$.
- Equation (10) defines a band-pass filter $F(s)$ used to extract the bias and the main oscillatory component.
- Equation (11) computes the RMS used to transform the main oscillation into a continuous variable.
- Equations (12)-(13) describe the control law, with input saturation. Note that this structure forces $u(t) \in [0, u_0], \forall t \geq 0$.

This scheme can be completed with an estimator for the main oscillation frequency, as shown in Figure 8.

We next summarize the rationality behind the OSKIL development (see [3] for further analysis).

Assume that the system under consideration has left its local attractive domain of operation, and as a consequence the state vector $x(t)$ has reached the stable orbit (limit-cycle). If the output $y(t)$ has been properly chosen, the oscillations are reflected on that measurement. As a consequence, we can then assume that $y(t)$ will be of the form

$$y(t) = y_0 + A_0\cos(\omega_0 t + \varphi_0) + \cdots$$

where y_0 is the bias component of the oscillation and A_0, $\omega_0 = \frac{2\pi}{T}$, φ_0 are the amplitude, frequency and phase of the main oscillatory component.

Using a filter of the form

$$F(s) = \frac{K_f s}{(s+\omega_1)(s+\omega_2)}$$

with $\omega_1 = \omega_0 - \Delta\omega > 0$, and $\omega_2 = \omega_0 + \Delta\omega > 0$, the output of (10), can be approximated as:

$$y_f(t) \approx A_0\cos(\omega_0 t + \varphi_1)$$

The value of K_f and $\Delta\omega$ are designed such that $|F(j\omega_0)| \approx 1$, and frequencies away from ω_0 are filtered out.

Equation (11) computes the RMS value of $y_f(t)$, yielding,

$$\xi = \int_t^{t+T} A_0^2\cos^2(\omega_0\tau + \varphi_1)d\tau \approx \frac{A_0^2 T}{2} \geq 0$$

This signal reflects the magnitude of the oscillation and it is suited to control oscillations. Note that in this computation,

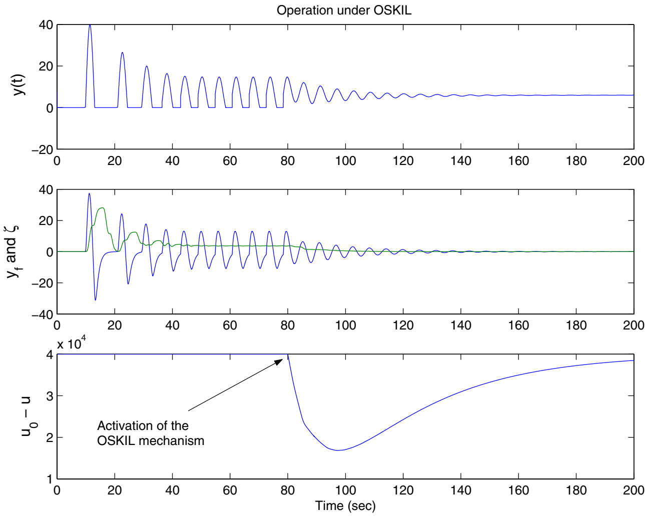

Fig. 9. Time profiles of the closed-loop solution of the drillstring. The output $y(t)$ (upper curves), the filtered signal $y_f(t)$, and its RMS value $\xi(t)$ (middle), and the evolution of $\tilde{u}(t)$ (lower). The OSKIL mechanism is activated at $t = 80sec$.

the exact value of T is not mandatory. For instance, if T is over estimated, the signal ξ will still reflect the amount of oscillation in the output y. Similar arguments apply if $|F(j\omega_0)| \neq 1$.

Equations (12)-(13) are for the purpose of producing a control signal bounded in the range $[0, u_0]$. The value of u should reflect the growth of ξ in this interval, with the property that if $\xi \to 0$, then $\tilde{u} \to 0$, hence that $u \to u_0$. This can be obtained by the proposed linear stable filter with input saturation. Further conditions on K_I are required to ensure that the desired equilibrium point is still the unique one. This can be reached by using sufficiently small K_I.

VI. Simulations

Simulation are carried out with the parameters shown in the appendix. Values of the gains are: $k_1 = 15278$, $k_2 = 33952$, $k_3 = 3468$. Figure 9 shows the time profiles of closed-loop signals of this example. As it can be observed with the nominal system $u_0 = 40000[Kg.m/s^2]$, the drillstring system exhibits stick-slip behavior of rotational drill bit velocity. The OSKIL mechanism is activated at $t = 80sec$. As it can be seen from the figures, the oscillations vanish while the WoB force recovers, as expected, its nominal drilling value.

VII. Conclusions

We have proposed to use the weight on the bit (**WoB**) force as an additional control variable to extinguish limit cycles when they occur. An adaptation, named D-OSKIL, of the *oscillation killer* (OSKIL) mechanism, to oil well drillstring systems has been proposed. An approximate analysis based on the bias describing function did provide a good insight on the slip-stick behavior and in the control design. Simulations applying the D-OSKIL mechanism have shown that the stick-slip oscillations can be indeed eliminated without requiring a re-design of the velocity rotary-table control. A formal stability analysis is currently under investigation.

Acknowledgments

The authors would like to acknowledge MCYT-FEDER for funding this work under grants DPI2004-06419, HF2003-0237 and SAB2003-0085. Thanks for funding are also due to the program PICASSO No. 07261YJ(EGIDE), of the French Minister of Foreign Affaires, the LAFMAA under CNRS-CONACYT grants and IMP project Y.00005.

Appendix

A. Simulation Parameters

$J_r = 2122$ $[Kg.m^2]$, $J_b = 374$ $[Kg.m^2]$, $M = 4000$ $[Kg]$, $c = 23.2$ $[1/s^2]$, $d_r = 425$ [1/s], $d_b = 50$ [1/s], $i = 1$, $k = 473$ $\mu_C = 0.3$, $\mu_S = 0.35$, $\sigma_0 = 25$ [1/rad], $\sigma_1 = 193$= [s/rad], $v_s = 0.01$ [rad/s], $u_0 = 40000$ $[Kg.m/s^2]$, $\omega_d = 6$ [rad/s], $K_f = 6$, $\omega_1 = 1$ [rad/s], $\omega_2 = 3$ [rad/s], $T = 5.8$ [s], $\sigma = 0.03$ [rad/s], $K_I = 3.16$.

References

[1] Abbasssian, F., Dunayevsky, V.A. Application of Stability Approach to Torsional and Lateral Bit Dynamics. *SPE Drilling and Completion*, 13(2):99–107, 1998.

[2] Atherton D.P. *Nonlinear Control Engineering. Describing Function: Analysis and Design.* Van Nostrand Reinhold, first edition, 1982.

[3] Canudas-de-Wit, C., Aracil, J., Gordillo, F., Salas, F. The oscillation killer: a mechanism to eliminate undersired oscillations in nonlinear systems. *Submitted to IEEE Conference on Decision and Control*, Feb-2005.

[4] Canudas-de-Wit, C., M. A. Corchero, F. R. Rubio and E. Navarro D-OSKIL: a New Mechanism for Suppressing Stick-Slip in Oil Well Drillstrings: complete report. *Internal report*, Feb-2005.

[5] Canudas-de-Wit C., Olsson H., Astrom K.J. and Lischinsky P. A new model for control of systems with friction. *IEEE Transactions on Automatic Control*, 40(3), 1995.

[6] Christoforou, A. P., Yigit, A. S. Fully coupled vibrations of actively controlled drilstrings. *Journal of Sound and Vibration*, 267:1029–1045, 2003.

[7] Halsey, G. W., Kyllingstad, A., Kylling, A. Torque Feedback Used to Cure Slip-stick Motion. *in the 63rd SPE Annual Technical Conference and Exhibition*, pages 277–282, 1988.

[8] Jansen, J. D., van den Steen, L. Active Damping of Self-excited Torsional Vibrations in Oil Well Drillstrings. *Journal of Sound and Vibration*, 179(4):647–668, 1995.

[9] Kyllingstad, A., Halsey, G. W. A Study of Slip-stick Motion of the Bit. *SPE Drilling Engineering*, pages 369–373, 1988.

[10] Leine R.I., van Campen D.H., Keultjes W.J.G. Stick-slip whirl interaction in drillstring dynamics. *Journal of Vibration and Acoustics*, 124:209–220, 2002.

[11] Navarro-López, E.M. and Suárez-Cortez, R. Modelling and analysis of stick-slip behaviour in a drillstring under dry friction. *Congress of the Mexican Association of Automatic Control*, pages 330–335, 2004.

[12] Navarro-López, E.M. and Suárez-Cortez, R. Practical approach to modelling and controlling stick-slip oscillations in oilwell drillstrings. *IEEE International Conference on Control Applications*, pages 1454–1460, 2004.

[13] Pavone D. R., Desplans J.P. Application of High Sampling Rate Downhole Measurements for Analysis and Cure of Stick-slip in Drilling. *in SPE Annual Technical Conference and Exhibition*, SPE 28324:335–345, 1994.

[14] Sananikone, P., Kamoshima, O., White, D.B. A Field Method for Controlling Drillstring Torsional Vibrations. *in IADC/SPE Drilling Conference*, IADC/SPE 23891:443–452, 1992.

[15] Serrarens A.F.A, van de Molengraft M.J.G., Kok J.J. and van den Steen L. H_∞ control for suppressing stick-slip in oil well drillstrings. *IEEE Control Systems Magazine*, 18(2), 1998.

[16] Spanos, P.D., Chavallier, A.M., Politis N.P. and Payne M.L. Oil well drilling: A vibrations perspective. *The Shock and Vibration Digest*, 35(2):81–99, 2003.